

Castration-induced Up-Regulation of Insulin-like Growth Factor Binding Protein-5 Potentiates Insulin-like Growth Factor-I Activity and Accelerates Progression to Androgen Independence in Prostate Cancer Models¹

Hideaki Miyake, Michael Pollak, and Martin E. Gleave²

The Prostate Centre, Vancouver General Hospital, Vancouver, British Columbia, V6H 3Z6 [H. M., M. E. G.]; Division of Urology, University of British Columbia, Vancouver, British Columbia V5Z 3J5 [H. M., M. E. G.]; and Lady Davis Research Institute of the Jewish General Hospital and Departments of Medicine and Oncology, McGill University, Montreal, Quebec, H3T 1E2 [M. P.], Canada

ABSTRACT

Although insulin-like growth factor binding protein-5 (IGFBP-5) has been shown to be implicated in prostate cancer progression, the functional role of IGFBP-5 in progression to androgen-independence remains largely undefined. Here, we demonstrate substantial up-regulation of IGFBP-5 during castration-induced regression and androgen-independent (AI) progression in the mouse androgen-dependent (AD) Shionogi tumor model. To analyze the functional significance of these changes in IGFBP-5, human AD LNCaP prostate cancer cells were stably transfected with *IGFBP-5* gene, and IGFBP-5-overexpressing LNCaP tumors progressed significantly faster to androgen independence after castration compared with controls. Antisense mouse IGFBP-5 oligodeoxynucleotides (ODNs) were then designed that reduced IGFBP-5 expression in Shionogi tumor cells *in vitro* in a dose-dependent and sequence-specific manner. Growth of Shionogi tumor cells was inhibited by antisense IGFBP-5 ODN treatment in a time- and dose-dependent manner, which could be reversed by exogenous IGF-I. However, antisense IGFBP-5 ODN treatment had no additive inhibitory effect on Shionogi tumor cell growth when IGF-I activity was neutralized by anti-IGF-I antibody. Antisense IGFBP-5 ODN treatment resulted in decreased mitogen-activated protein kinase activity and number of cells in the S + G₂-M phases of the cell cycle that directly correlated with reduced proliferation rate of Shionogi tumor cells. Systemic administration of antisense IGFBP-5 ODN in mice bearing Shionogi tumors after castration significantly delayed time to progression to androgen independence and inhibited growth of AI recurrent tumors. These findings suggest that up-regulation of IGFBP-5 after castration serves to enhance IGF bioactivity and raise the possibility that the response of prostate cancer to androgen withdrawal can be enhanced by strategies, such as antisense IGFBP-5 ODN therapy, that target IGF signal transduction.

INTRODUCTION

No therapy surpasses androgen withdrawal in patients with advanced prostate cancer. Approximately 80% of patients initially respond to this therapy; however, progression to androgen independence ultimately occurs and represents the major obstacle to effective control and cure of advanced disease (1). Although novel nonhormonal therapies have been evaluated in patients with AI³ disease, none of these agents have improved survival (2). A more rational strategy, therefore, would involve earlier application of novel agents designed to target the molecular mechanisms mediating AI progression to delay the emergence to the AI phenotype.

IGF-I and IGF-II are potent mitogens and antiapoptotic factors for many normal and malignant tissues. The biological response of cells to IGFs is regulated by various factors in the microenvironment, including the IGFBPs (3). To date, at least six IGFBPs have been identified that modulate the biological action of the IGFs through high-affinity binding interactions that influence the ability of IGFs to function as ligands for the type I IGF receptor (4). However, IGFBP physiology is complex, as evidenced by the fact that both stimulatory and inhibitory effects of IGFBPs on cell proliferation have been reported (5–8) and also data suggesting that certain regulatory actions of IGFBPs are independent of IGFs (4, 5, 9). Additional complexity is suggested by data documenting that an IGFBP-related protein has tumor suppressor activity for prostate cancer (10).

Accumulating evidence suggests that the IGF system plays an important role in the pathophysiology of cell turnover and renewal in the prostate. In the normal prostate, IGFs are produced by epithelial and stromal cells, and both IGF-I and IGF-II are mitogenic for epithelial cells (11). Furthermore, in prostate cancer cells, autocrine stimulation by both IGF-I and IGF-II has been demonstrated (12). Several IGFBPs are produced by normal prostate epithelial and/or stromal cells, and after castration or treatment with antiandrogens, the expression levels of certain IGFBPs are rapidly and significantly altered (13–17). Changes in expression of various IGFBPs in benign and malignant prostatic epithelial cells have also been reported, with an increase in IGFBP-2 and IGFBP-5 and decrease in IGFBP-3 from benign to malignant state (18). The functional significance of these changes in *IGFBP* gene expression has not been established.

Controlled study of the complex molecular processes associated with AI progression in prostate cancer has proved difficult because few animal models exist that mimics the clinical course of the disease in men. The Shionogi tumor model is an AD mouse mammary carcinoma xenograft that grows s.c. in male syngeneic hosts. In this model, AD tumors in male mice undergo complete regression after castration but recur as rapidly growing AI tumors after 1 month (19). The highly reproducible regression and recurrence pattern provides a reliable end point to test the efficacy of agents targeting castration-induced apoptosis and their effects on time to AI progression. Of the currently available human prostate cancer cell lines, only the LNCaP cell line is AD, PSA-secreting, and immortalized *in vitro*. As in human prostate cancer, serum PSA levels in the LNCaP tumor model are initially regulated by androgen and directly proportional to tumor volume, with loss of androgen-regulated *PSA* gene expression after castration as a surrogate end point of AI progression (20). Therefore, both the Shionogi and LNCaP tumor models are particularly useful in studying mechanisms controlling castration-induced apoptosis and AI progression.

In this study, to investigate the functional significance of IGFBP-5 up-regulation after castration and during AI progression, we first evaluated the effects of IGFBP-5 overexpression by stable transfection on time to AI progression in the LNCaP tumor model and then tested the effects of antisense IGFBP-5 ODN on Shionogi tumor growth both *in vitro* and *in vivo*. Up-regulation of IGFBP-5 expression

Received 7/30/99; accepted 3/31/00.

The costs of publication of this article were defrayed in part by the payment of page charges. This article must therefore be hereby marked *advertisement* in accordance with 18 U.S.C. Section 1734 solely to indicate this fact.

¹ This work was supported by Grant 009002 from the National Cancer Institute of Canada.

² To whom requests for reprints should be addressed, at Division of Urology, University of British Columbia, D-9, 2733 Heather Street, Vancouver, British Columbia, V5Z 3J5 Canada.

³ The abbreviations used are: AI, androgen independent; AD, androgen dependent; IGF, insulin-like growth factor; ODN, oligodeoxynucleotide; IGFBP, insulin-like growth factor binding protein; PSA, prostate-specific antigen; CMV, cytomegalovirus; MAPK, mitogen-activated protein kinase; G3PDH, glyceraldehyde-3-phosphate dehydrogenase; MTT, 3-(4,5-dimethylthiazol-2-yl)-2,5-diphenyltetrazolium bromide.

associated with steroid hormone deprivation had been hypothesized previously to reduce IGF activity and thereby contribute to induction of apoptosis (21). However, our findings demonstrate that increased IGFBP-5 expression after castration represents an adaptive response to enhance IGF bioactivity, which functions to accelerate time to emergence of an AI phenotype.

MATERIALS AND METHODS

Expression Plasmid and Transfection to LNCaP Cells. LNCaP cells were kindly provided by Dr. Leland W. K. Chung (University of Virginia, Charlottesville, VA) and maintained in RPMI 1640 (Life Technologies, Inc., Gaithersburg, MD) supplemented with 5% heat-inactivated FCS. pRC-CMV expression vector containing the cDNA fragment encoding human *IGFBP-5* was transfected into LNCaP cells by the liposome-mediated gene transfer method (22). Briefly, 2×10^5 LNCaP cells were plated in six-cm plates. The next day, 5 μ g of purified *IGFBP-5* cloned pRC-CMV or pRC-CMV alone (as a control) were added to LNCaP cells after a preincubation for 30 min with 5 μ g of Lipofectamine reagent and 3 ml of serum-free OPTI-MEM (Life Technologies, Inc.). Drug selection, in 300 μ g/ml Geneticin (Sigma Chemical Co., St. Louis, MO), was begun 3 days after the transfection. Colonies were harvested 2 weeks after drug selection using cloning cylinders, and cell lines were expanded for *in vivo* injection.

Assessment of *in Vivo* LNCaP Tumor Growth and Determination of Serum PSA Levels. One million cells of each LNCaP subline were inoculated s.c. with 0.1 ml of Matrigel (Becton Dickinson Labware, Lincoln Park, NJ) in the flank region of 6–8-week-old male athymic nude mice (BALB/c strain; Charles River Laboratory, Montreal, Quebec, Canada). Each experimental group consisted of six mice. Mice were castrated via a scrotal approach when tumors reached 100 and 200 mm³ in volume. Tumor volume was measured once weekly and calculated by the formula length \times width \times depth \times 0.5236 (20). Blood samples were obtained with tail vein incisions of mice once weekly. Serum PSA levels were determined by an enzymatic immunoassay kit with a lower limit of sensitivity of 0.2 μ g/l (Abbott IMX, Montreal, Quebec, Canada) according to the manufacturer's protocol. Data points were reported as mean values \pm SD.

Shionogi Tumor Growth. The Toronto subline of the transplantable SC-115 AD mouse mammary carcinoma (23) was used in all experiments. Shionogi tumor cells were maintained in DMEM (Life Technologies, Inc.) supplemented with 5% heat-inactivated FCS. For *in vivo* study, approximately 5×10^6 cells of the Shionogi carcinoma were injected s.c. into adult male DD/S strain mice. When Shionogi tumors became 1–2 cm in diameter, usually 2–3 weeks after injection, castration was performed through an abdominal incision under methoxyflurane anesthesia. Mice required sacrifice when tumor mass increased >3 cm³ or 10% of body weight in accordance with institutional accredited guidelines. Details of the maintenance of mice, tumor stock, and operative procedures are described in a previous publication (24).

Antisense IGFBP-5 ODN. Phosphorothioate ODNs used in this study were obtained from Nucleic Acid-Protein Service Unit, University of British Columbia (Vancouver, Canada). The sequences of antisense IGFBP-5 ODN corresponding to the mouse IGFBP-5 translation initiation site were 5'-GAC-CACGCTGATCACCAT-3'. Two base IGFBP-5 mismatch ODNs (5'-GAC-CACGCTCATGACCAT-3') were used as control.

Treatment of Cells with ODN. Lipofectin, a cationic lipid (Life Technologies, Inc.), was used to increase the ODN uptake of cells. Shionogi cells were treated with various concentrations of ODN after a preincubation for 20 min with 4 μ g/ml lipofectin in serum-free OPTI-MEM (Life Technologies, Inc.). Four h after the beginning of the incubation, the medium containing ODN and lipofectin was replaced with standard culture medium described above.

Northern Blot Analysis. Total RNA was isolated from Shionogi tumor tissues and cultured Shionogi tumor cells by the acid-guanidinium thiocyanate-phenol-chloroform method. The electrophoresis, hybridization, and washing conditions were carried out as reported previously (19). Mouse IGFBP-5 and G3PDH cDNA probes were generated by reverse transcription-PCR from total RNA of mouse brain using primers 5'-AGAAAATGGTATCAGCGTGGT-3' (sense) and 5'-TTCGGATTCTGTCTCATCTCA-3' (antisense) for IGFBP-5, and 5'-ATGGTGAAGGTGGTGTGA-ACGGAT-3' (sense) and 5'-AAAGTTGTCATGGATGACCTT-3' (antisense) for G3PDH. Density of

bands for IGFBP-5 was normalized against that of G3PDH by densitometric analysis.

MTT Assay. The *in vitro* effects of antisense IGFBP-5 ODN, anti-IGF-I antibody (Upstate Biotechnology, Lake Placid, NY), and/or recombinant IGF-I (Sigma Chemical Co.) on growth of Shionogi tumor cells were assessed by the MTT assay as described previously (22). Briefly, 1×10^4 cells were seeded in each well of 96-well microtiter plates and allowed to attach overnight. Cells were then treated once daily with various concentrations of ODN for 2 days in the media containing 5 nM recombinant IGF-I or 10 μ g/ml anti-IGF-I antibody. Forty-eight h after ODN treatment, 20 μ l of 5 mg/ml MTT (Sigma Chemical Co.) in PBS were added to each well, followed by incubation for 4 h at 37°C. The formazan crystals were then dissolved in DMSO. The absorbance was determined with a microculture plate reader (Becton Dickinson Labware, Lincoln Park, NJ) at 540 nm. Absorbance values were normalized to the values obtained for the vehicle-treated cells to determine the percentage of survival. Each assay was performed in triplicate.

Cell Death Assay. Shionogi tumor cells were treated as described above. Live and dead cells from each subculture of cells were counted using trypan blue 48 h after ODN treatment, and the ratio of dead/total cells was calculated. Each assay was performed in triplicate.

MAPK *in Vitro* Kinase Assay. Shionogi tumor cells were treated as described above, and MAPK activity was measured using a MAP Kinase Assay Kit (New England Biolabs, Beverly, MA). Briefly, the cells were washed with PBS, lysed in lysis buffer, sonicated, and microcentrifuged for 20 min at 4°C. The supernatants was incubated with 1:100-diluted anti-phospho-MAPK antibody for 4 h. Protein A-agarose beads were then added and incubated for another 3 h. The pellets were washed twice with ice-cold lysis buffer and twice with kinase buffer. The pellets were incubated with 100 mM ATP and 20 mg/ml Elk1 fusion protein, a substrate of MAPK, for 30 min at 30°C. Samples were boiled, separated by electrophoresis through a 10% SDS-polyacrylamide gel, and transferred to polyvinylidene difluoride membranes. The membranes were incubated for 1 h at room temperature in blocking buffer and then probed with 1:1000-diluted anti-phospho-Elk1 antibody. After being washed, the membranes were incubated with a 1:1000-diluted horseradish peroxidase-conjugated antirabbit immunoglobulin (Amersham Life Science, Arlington Heights, IL). The immunoreactivity of phosphorylated Elk1 was determined using an ECL chemiluminescence kit (Amersham Life Science).

Flow Cytometric Analysis. The flow cytometric analysis of propidium iodide-stained nuclei was performed as described previously (22). Briefly, Shionogi tumor cells were plated at a density of 5×10^6 cells in six-cm dishes and treated as described above. The cells were trypsinized 48 h after ODN treatment, washed twice with PBS, and fixed in 70% ethanol for 5 h at 4°C. The fixed cells were washed twice with PBS, incubated with 1 μ g/ml RNaseA (Sigma Chemical Co.) for 1 h at 37°C, and stained with 5 μ g/ml propidium iodide (Sigma Chemical Co.) for 1 h at room temperature. The stained cells were analyzed for relative DNA content on a FACScan (Becton Dickinson Labware).

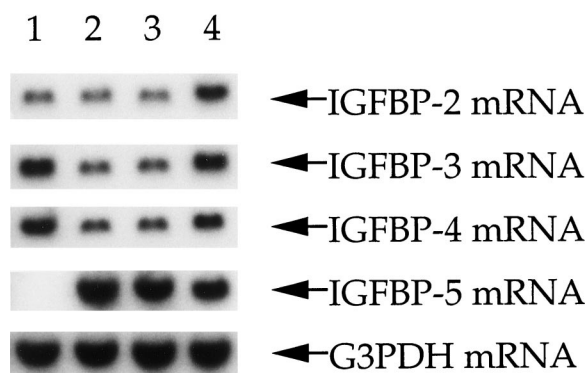


Fig. 1. Changes of IGFBP mRNA expression in the Shionogi tumor model. Shionogi tumors were harvested before and at several time points after castration; total RNA was extracted from each tumor tissue and analyzed for IGFBP-2, IGFBP-3, IGFBP-4, IGFBP-5, and G3PDH levels by Northern blotting. Lane 1, AD tumor before castration; Lane 2, regressing tumor 4 days after castration; Lane 3, regressing tumor 7 days after castration; Lane 4, AI recurrent tumor 28 days after castration.

In Vivo ODN Treatment. Male DD/S mice bearing Shionogi tumors were castrated and randomly selected for treatment with antisense IGFBP-5 versus mismatch control ODN. Each experimental group consisted of eight mice. Beginning the day of castration, 15 mg/kg antisense IGFBP-5 or mismatch control ODNs were injected i.p. once daily into each mouse for 50 days. Tumor volume was measured twice weekly and calculated as described above. Data points were reported as average tumor volumes \pm SD.

RESULTS

Changes of IGFBPs mRNA Expression in the Shionogi Tumor Model. Northern blot analyses were used to characterize changes in IGFBPs mRNA expression in AD intact tumors before castration, regressing tumors 4 and 7 days after castration, and AI recurrent tumors 28 days after castration. As shown in Fig. 1, various patterns of changes in IGFBP-2, IGFBP-3, IGFBP-4, and IGFBP-5 mRNA expression were observed. IGFBP-1 and IGFBP-6 mRNAs are undetectable in the Shionogi tumor model (data not shown). Of the remaining IGFBPs, the most dramatic changes in expression were observed with IGFBP-5. We confirmed our prior observation (25) that IGFBP-5 expression is undetectable in AD intact tumors and highly up-regulated after castration. In addition, Fig. 1 illustrates that IGFBP-5 expression remains high in AI tumors. The observed pattern of IGFBP-5 up-regulation in the Shionogi tumor model during AI progression is similar to that in rat prostate (13) and human prostate (18) cancer.

Overexpression of IGFBP-5 Accelerates Time to AI Progression after Castration in the LNCaP Tumor Model. To determine the effects of IGFBP-5 overexpression on time to AI progression after androgen ablation, LNCaP cells were transfected with *IGFBP-5* cDNA expression vector pRC-CMV/IGFBP-5 or the pRC-CMV vector alone as a control. As shown in Fig. 2A, abundant levels of IGFBP-5 mRNA were detected in four independent IGFBP-5-transfected clones (LNCaP/IGFBP-5#1 to LNCaP/IGFBP-5#4), whereas the control vector-transfected cell line (LNCaP/Co) did not express detectable IGFBP-5 mRNA levels. LNCaP/Co, LNCaP/IGFBP-5#1, and LNCaP/IGFBP-5#2 were selected for *in vivo* study, with 1×10^6 of each cell line inoculated s.c. in intact male nude mice. No difference in tumor take rates, tumor volume, or serum PSA levels were apparent between different LNCaP sublines grown in intact nude mice prior to castration. After castration, LNCaP/Co tumor growth was inhibited for 4 weeks, after which LNCaP/Co tumor volume increased 2.0-fold by 8 weeks after castration. In contrast, LNCaP/IGFBP-5#1 and LNCaP/IGFBP-5#2 tumor volume continued to grow after castration, increasing 4.3- and 5.1-fold, respectively, by 8 weeks after castration (Fig. 2B). Serum PSA in mice bearing LNCaP/Co tumors decreased by 76% by 2 weeks after castration and increased from 4 to 8 weeks after castration by 1.3-fold. In comparison, serum PSA in mice bearing LNCaP/IGFBP-5#1 and LNCaP/IGFBP-5#2 tumors decreased by 61 and 59%, respectively, before increasing beginning 2 weeks after castration to 3.7- and 4.2-fold, respectively, by 8 weeks (Fig. 1C).

Antisense ODN-mediated Inhibition of IGFBP-5 Expression in Shionogi Tumor Cells. The effect of treatment with antisense IGFBP-5 ODN on IGFBP-5 mRNA expression in Shionogi tumor cells was initially evaluated by Northern blot analysis. As shown in Fig. 3A and B, daily treatment of Shionogi tumor cells with antisense IGFBP-5 ODN (50, 100, 500, or 1000 nm) for 2 days reduced IGFBP-5 mRNA levels by 0, 7, 54, or 83%, respectively, whereas IGFBP-5 mRNA expression was not affected by the two-base mismatch control ODN at any of the concentrations used.

To further analyze the specificity of antisense IGFBP-5 ODN, Northern blotting was performed after treatment of Shionogi tumor

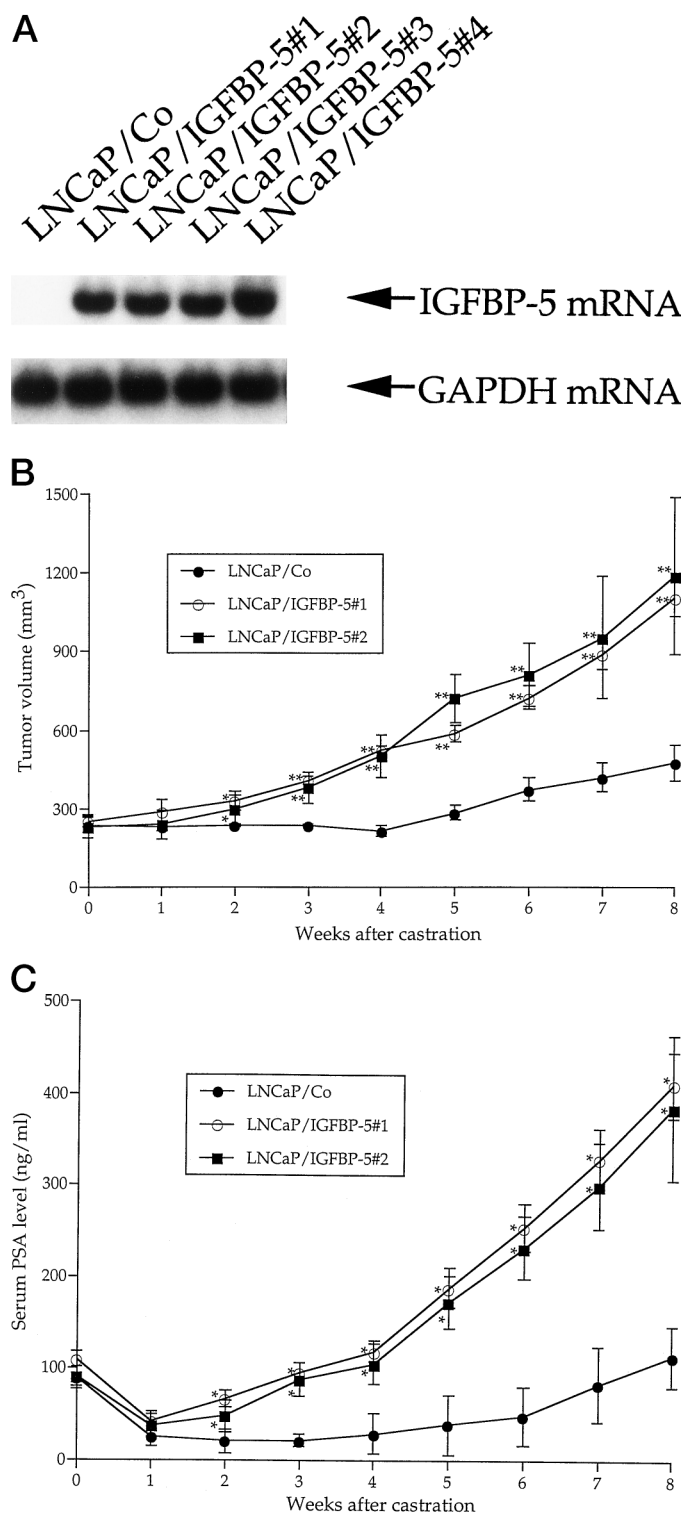


Fig. 2. Effect of IGFBP-5 overexpression on LNCaP tumor growth and serum PSA levels in nude mice after castration. **A**, total RNA was extracted from LNCaP/Co and four clones of IGFBP-5 transfectants (LNCaP/IGFBP-5#1 to LNCaP/IGFBP-5#4) and analyzed for IGFBP-5 and GAPDH levels by Northern blotting. **B**, each LNCaP subline was injected s.c. into male nude mice, and after castration, tumor volume was measured once weekly. Each point represents the mean tumor volume in each experimental group containing six mice; bars, SD. * and **, significantly different from LNCaP/Co: $P < 0.05$ and 0.01 (Student's *t* test), respectively. **C**, blood samples for measurement of serum PSA levels were obtained with tail vein of the mice after castration once weekly. Serum PSA levels were determined by an enzymatic immunoassay kit according to the manufacturer's control (Abbott IMX, Montreal, Quebec, Canada). Each point represents the mean PSA level in each experimental group containing six mice; bars, SD. *, significantly different from LNCaP/Co: $P < 0.01$ (Student's *t* test).

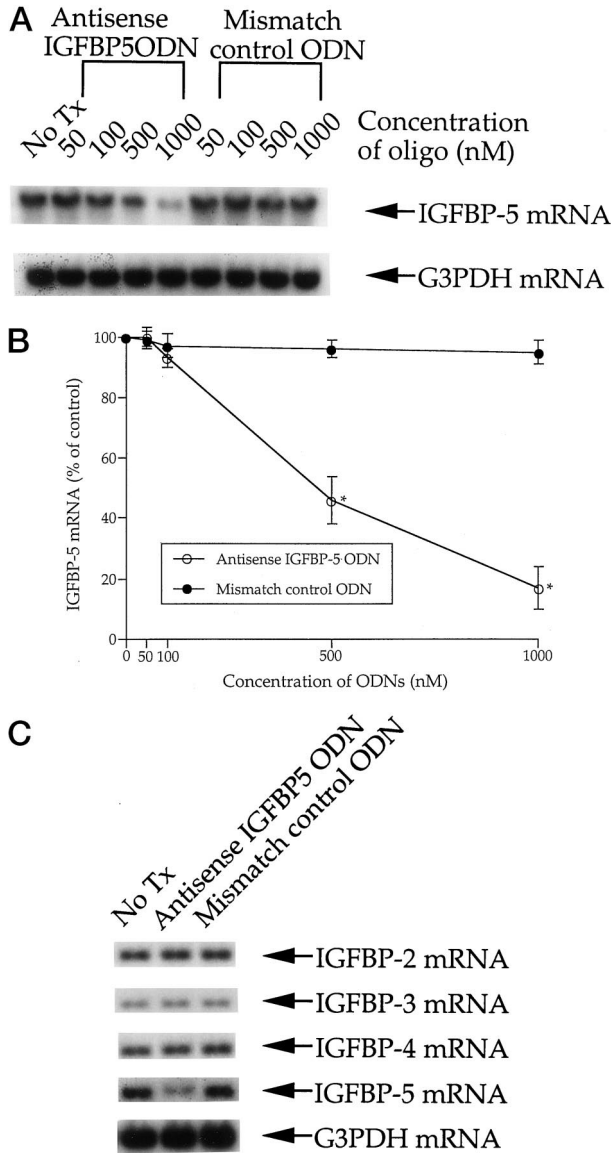


Fig. 3. Sequence-specific inhibition of IGFBP-5 mRNA by antisense IGFBP-5 ODN in Shionogi tumor cells. **A**, Shionogi tumor cells were treated once daily with various concentrations of antisense IGFBP-5 ODN (GACCACGCTGATCACCAT) or a two-base IGFBP-5 mismatch ODN (GACCACGCTCATGACCAT) as a control for 2 days. Total RNA was then extracted from culture cells and analyzed; IGFBP-5 and G3PDH levels were analyzed by Northern blotting. *No Tx*, untreated cells. **B**, quantitative analysis of IGFBP-5 mRNA levels after normalization to G3PDH mRNA levels in Shionogi tumor cells after treatment with various concentrations of antisense IGFBP-5 or mismatch control ODN was performed by using laser densitometer. Each *point* represents the mean of triplicate analyses; *bars*, SD. *, significantly different from mismatch control ODN treatment: $P < 0.01$ (Student's *t* test). **C**, Northern blot analysis of IGFBP-2, IGFBP-3, IGFBP-4, IGFBP-5, and G3PDH mRNA levels in Shionogi tumor cells daily treated with $1 \mu\text{M}$ antisense IGFBP-5 or mismatch control ODN for 2 days was performed. *No Tx*, untreated cells.

cells with $1 \mu\text{M}$ antisense IGFBP-5 ODN to quantify changes in expression of other *IGFBP* (*IGFBP-2*, *IGFBP-3*, and *IGFBP-4*) genes, which share significant sequence homology with *IGFBP-5*. Although antisense IGFBP-5 ODN markedly reduced IGFBP-5 mRNA expression, no effects were observed on IGFBP-2, IGFBP-3, and IGFBP-4 expression levels (Fig. 3C). Collectively, these data demonstrate that antisense IGFBP-5 ODN used in this study induces sequence-specific, gene-specific, and dose-dependent down-regulation of its target gene.

Antiproliferative Effects of Antisense IGFBP-5 ODN on Shionogi Tumor Cells. To determine the effects of antisense IGFBP-5 ODN on cell proliferation, we treated Shionogi tumor cells

once daily with either $1 \mu\text{M}$ antisense IGFBP-5 or mismatch control ODN for 2 days and determined cell number over a 72-h period. Antisense IGFBP-5 ODN treatment of cells resulted in significant inhibition of Shionogi tumor cell proliferation over this 72 h, whereas cell growth was not influenced by treatment with mismatch control ODN (Fig. 4A).

The effects of antisense IGFBP-5 ODN on cell proliferation were

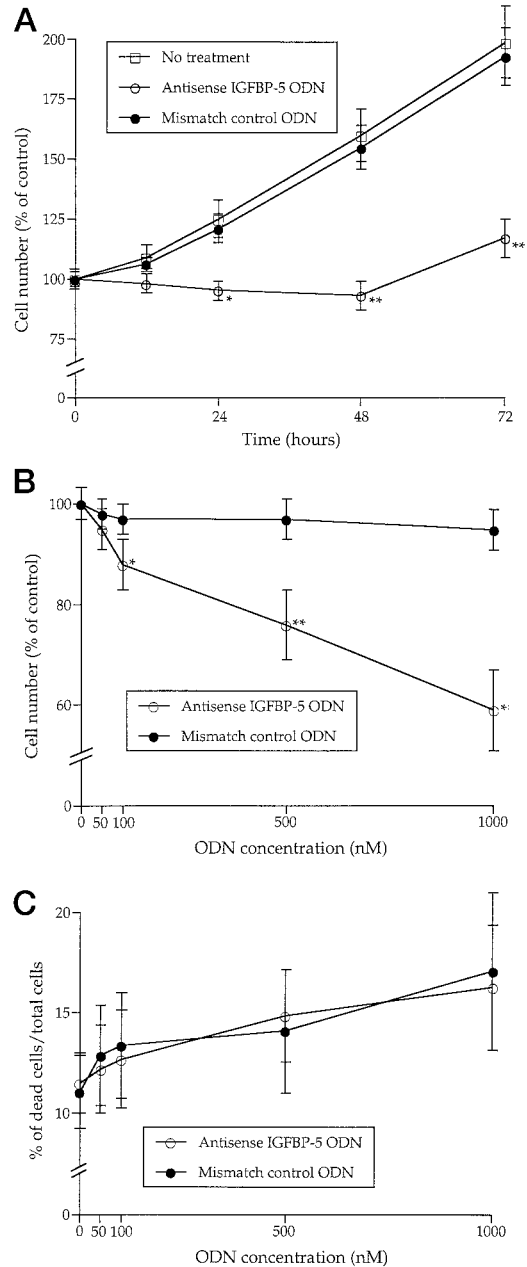


Fig. 4. Effects of antisense IGFBP-5 ODN treatment on Shionogi tumor cell growth. **A**, Shionogi tumor cells were treated once daily with $1 \mu\text{M}$ antisense IGFBP-5 ODN or mismatch control ODN for 2 days. After ODN treatment, cell viability was determined over a 72-h period by MTT assay. Each *point* represents the mean of triplicate analyses; *bars*, SD. * and **, significantly different from mismatch control ODN treatment: $P < 0.05$ and 0.01 , respectively (Student's *t* test). **B**, Shionogi tumor cells were treated once daily with various concentrations of antisense IGFBP-5 ODN or mismatch control ODN for 2 days, and 48 h after ODN treatment, cell viability was determined by MTT assay. Each *point* represents the mean of triplicate analyses; *bars*, SD. * and **, significantly different from mismatch control ODN treatment: $P < 0.05$ and 0.01 , respectively (Student's *t* test). **C**, Shionogi tumor cells were treated once daily with various concentrations of antisense IGFBP-5 ODN or mismatch control ODN for 2 days, and 48 h after ODN treatment, the numbers of live and dead cells were determined by cell death assay. Each *point* represents the mean of triplicate analyses; *bars*, SD.

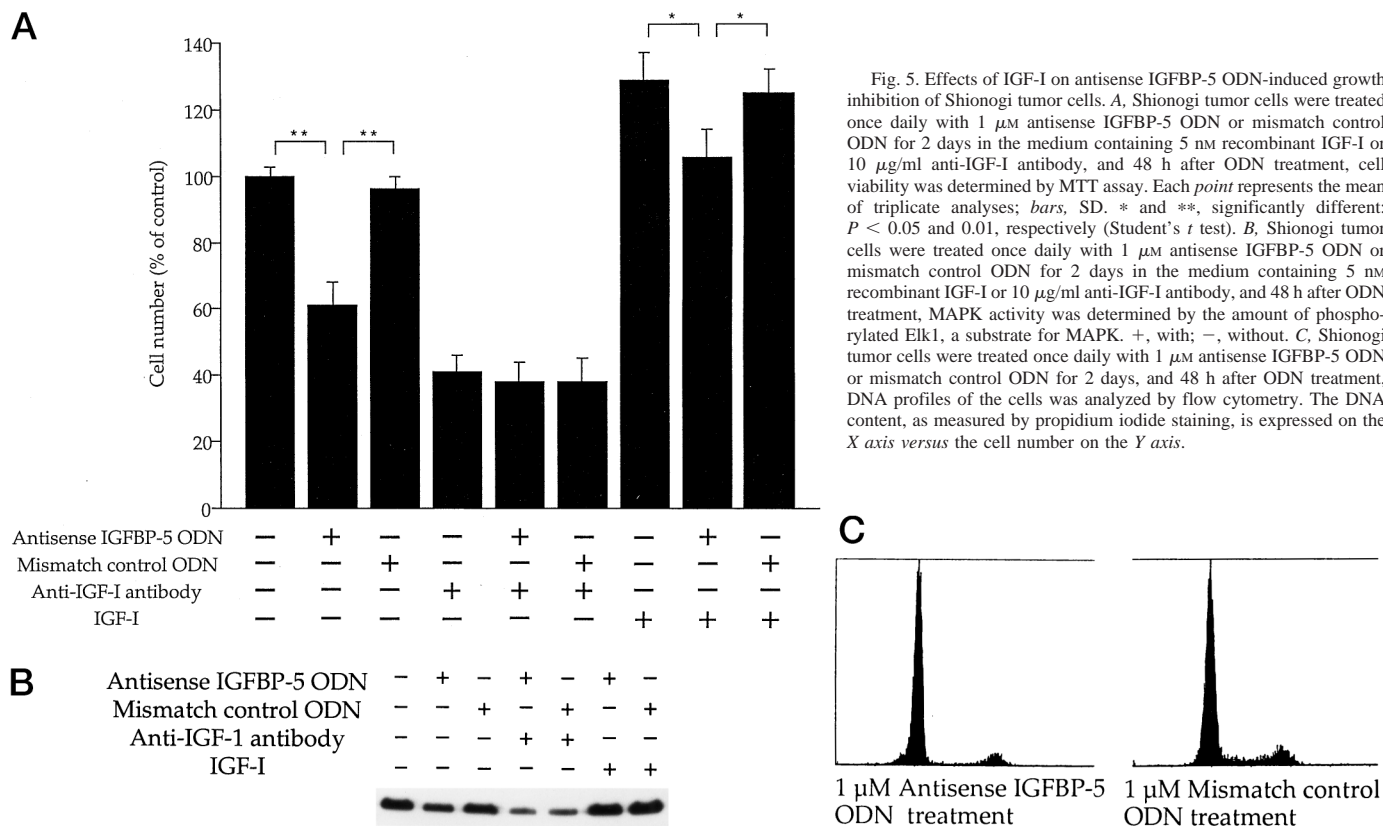


Fig. 5. Effects of IGF-I on antisense IGFBP-5 ODN-induced growth inhibition of Shionogi tumor cells. **A**, Shionogi tumor cells were treated once daily with 1 μ M antisense IGFBP-5 ODN or mismatch control ODN for 2 days in the medium containing 5 nM recombinant IGF-I or 10 μ g/ml anti-IGF-I antibody, and 48 h after ODN treatment, cell viability was determined by MTT assay. Each point represents the mean of triplicate analyses; bars, SD. * and **, significantly different: $P < 0.05$ and 0.01 , respectively (Student's *t* test). **B**, Shionogi tumor cells were treated once daily with 1 μ M antisense IGFBP-5 ODN or mismatch control ODN for 2 days in the medium containing 5 nM recombinant IGF-I or 10 μ g/ml anti-IGF-I antibody, and 48 h after ODN treatment, MAPK activity was determined by the amount of phosphorylated Elk1, a substrate for MAPK. +, with; -, without. **C**, Shionogi tumor cells were treated once daily with 1 μ M antisense IGFBP-5 ODN or mismatch control ODN for 2 days, and 48 h after ODN treatment, DNA profiles of the cells was analyzed by flow cytometry. The DNA content, as measured by propidium iodide staining, is expressed on the X axis versus the cell number on the Y axis.

also found to be dose dependent over a concentration range between 100 and 1000 nM (Fig. 4B). These antiproliferative effects directly correlated with the degree of IGFBP-5 mRNA reduction in Shionogi tumor cells by antisense IGFBP-5 ODN. In contrast, no significant effects were observed on cell proliferation treated with mismatch control ODN at any of the used concentrations.

To determine whether a decrease in cell proliferation by antisense IGFBP-5 ODN resulted from apoptosis, the number of live and dead cells were counted after antisense IGFBP-5 or mismatch control ODN treatment. The ratio of dead cells to total cell number of antisense IGFBP-5 ODN-treated cells was not significantly different from that of mismatch control ODN-treated cells (Fig. 4C). Hence, inhibition of cell growth after antisense IGFBP-5 ODN treatment is not the result of enhanced apoptosis.

IGF-I-dependent Effects of Antisense IGFBP-5 ODN on Shionogi Tumor Cells. To analyze the relationship between IGFBP-5 and IGF-I in the regulation of Shionogi tumor cell growth, the effects of antisense IGFBP-5 ODN treatment on the cell growth in the presence of anti-IGF-I antibody and/or recombinant IGF-I were evaluated. As shown in Fig. 5A, recombinant IGF-I increased Shionogi tumor cell growth, whereas anti-IGF-I antibody inhibited the cell growth. Furthermore, exogenous recombinant IGF-I treatment could overcome the inhibitory effects on the cell growth by antisense IGFBP-5 ODN. Treatment of Shionogi cells with antisense IGFBP-5 ODN and anti-IGF-I antibody did not produce additive growth-inhibitory effects over that of anti-IGF-I antibody alone. These findings support an enhancing and IGF-I-dependent effect of IGFBP-5 on the cell proliferation.

Because MAPK is one of the most potent pathways for IGF-I signal transduction (26), we evaluated the effects of antisense IGFBP-5 ODN with anti-IGF-I antibody or recombinant IGF-I on MAPK activity in Shionogi tumor cells. Changes in MAPK activity were directly related to changes in cell proliferation induced by these agents. Specifically, antisense IGFBP-5 ODN reduced MAPK activity,

the antisense IGFBP-5-induced reduction of MAPK activity could be overcome by recombinant IGF-I, and antisense IGFBP-5 had no additional inhibitory effect on MAPK activity when the mitogenic effects of IGF-I were neutralized by anti-IGF-I antibody (Fig. 5B).

To examine effects of changes in IGFBP-5 expression levels on cell cycle regulation, flow cytometric analysis was performed in Shionogi tumor cells. As shown in Fig. 5C, decreases in IGFBP-5 expression levels induced by antisense IGFBP-5 ODN treatment resulted in G₁ cell cycle arrest, thereby reducing the fraction of cells in the S + G₂-M phases by >50% compared with mismatch control ODN treatment.

Antisense IGFBP-5 ODN Delays AI progression of Shionogi Tumors in Vivo. Male mice bearing Shionogi tumors were castrated 2-3 weeks after tumor implantation, at which time tumors were 1-2 cm in diameter and randomly selected for treatment with antisense IGFBP-5 versus mismatch control ODN. Mean tumor volume was similar in both groups at the beginning of ODN treatment. Beginning the day of castration, 15 mg/kg ODN was administered once daily by i.p. injection for 50 days. As shown in Fig. 6A, antisense IGFBP-5 ODN treatment delayed recurrence of AI tumors compared with mismatch control ODN treatment. Although AI tumors recurred in all mice in both groups during an observation period of 60 days after castration, the median time to emergence of first palpable AI recurrent tumors was delayed by 7 days in mice treated with antisense IGFBP-5 ODN (35 days after castration) compared with that in mice treated with mismatch control ODN (28 days after castration). Furthermore, growth of recurrent AI tumors was substantially inhibited in the antisense IGFBP-5 ODN treatment group compared with the mismatch control ODN group, and the time to sacrifice of mice was significantly prolonged in the antisense IGFBP-5 ODN treatment group, i.e., all mice required sacrifice in mismatch ODN group after a median of 53 days after castration compared with only one of eight mice in the antisense IGFBP-5 ODN treatment group 60 days after castration.

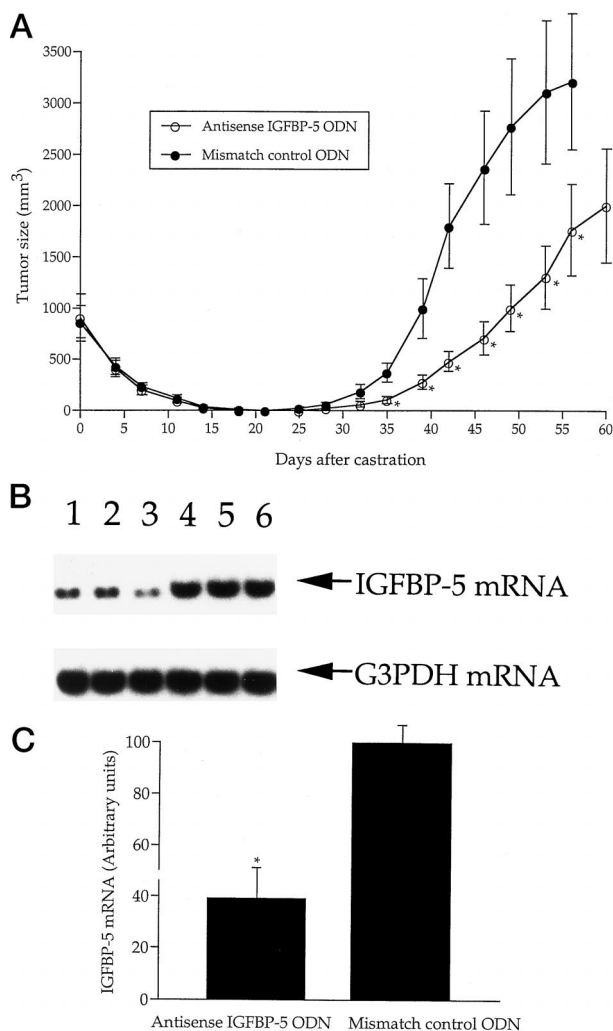


Fig. 6. Effects of antisense IGFBP-5 ODN administration on Shionogi tumor growth. *A*, beginning the day of castration, 15 mg/kg antisense IGFBP-5 or mismatch control ODN was injected i.p. once daily for 50 days into each mouse bearing Shionogi tumors. Tumor volume was measured twice weekly and calculated by the formula: length \times width \times depth \times 0.5236. Each point represents the mean tumor volume in each experimental group containing eight mice; bars, SD. *, significantly different from mismatch control ODN treatment: $P < 0.01$ (Student's *t* test). *B*, beginning the day of castration, each of three Shionogi tumor-bearing mice were daily treated with antisense IGFBP-5 or mismatch control ODN at a dose of 15 mg/kg; total RNA was extracted from Shionogi tumors 3 days after castration, and IGFBP-5 and G3PDH mRNA levels were analyzed by Northern blotting. Lanes 1–3, Shionogi tumors in mice administered antisense IGFBP-5 ODN; Lanes 3–5, Shionogi tumors in mice administered mismatch control ODN. *C*, quantitative analysis of IGFBP-5 mRNA levels after normalization to G3PDH mRNA levels in Shionogi tumors after treatment with antisense IGFBP-5 or mismatch control ODN was performed by using laser densitometer. Each column represents the mean value; bars, SD. *, significantly different from mismatch control ODN treatment: $P < 0.01$ (Student's *t* test).

The effects of *in vivo* ODN treatment on IGFBP-5 mRNA expression in Shionogi tumors were measured by Northern blotting. In this experiment, beginning the day of castration, each of three tumor-bearing mice were administered 15 mg/kg antisense IGFBP-5 or mismatch control ODN i.p. once daily, and tumor tissues were harvested for RNA extraction 3 days after castration. Antisense IGFBP-5 ODN resulted in a 61% reduction in IGFBP-5 mRNA levels in Shionogi tumors compared with mismatch control ODN-treated tumors (Fig. 6, *B* and *C*).

DISCUSSION

Previous studies have identified a strong association between the IGF system and prostate cancer progression. Examples include cell

biology data demonstrating autocrine growth stimulation of prostate cancer cells by IGFs (12, 26) and epidemiological data showing a strong positive correlation between circulating IGF-I levels and prostate cancer risk (27). Changes in IGFBP expression levels in normal prostate have also been observed after androgen ablation (13–17). Collectively, these findings suggest a possible functional role for IGFBPs in prostate cancer after androgen withdrawal and during AI progression.

Recently, we reported a dramatic increase in IGFBP-5 expression after castration in the Shionogi tumor model, and that IGFBP-5 expression is directly regulated by apoptosis-inducing stimuli rather than androgen (25). Our results agree with previous findings that IGFBP-5 expression changes most substantially among several IGFBPs in prostate tissues after androgen withdrawal (13–17). Although various functional roles of IGFBP-5 expression have been suggested in different model systems, these data are varying and conflicting. For example, IGFBP-5 has been reported to either stimulate or inhibit cell proliferation under different experimental conditions (4–6, 28–31), and these effects are exerted dependent and/or independent of its well-characterized actions associated with modulation of IGF bioavailability (4, 5). Furthermore, to date, there has been no data demonstrating the functional significance of IGFBP-5 up-regulation after androgen ablation in prostate cancer progression.

In this study, we generated several IGFBP-5-overexpressing LNCaP cell lines to characterize the functional role of IGFBP-5 up-regulation in AI progression of prostate cancer. Although tumor incidence, tumor growth rates, and serum PSA levels were similar among the LNCaP sublines growing in intact mice, tumor growth and serum PSA levels increased severalfold faster in mice bearing IGFBP-5-transfected LNCaP tumors after castration than those bearing control LNCaP tumors. These results provide the first clear evidence that IGFBP-5 up-regulation in prostate cancer cells after castration accelerates time to AI progression.

To further define the functional significance of IGFBP-5 up-regulation after castration, we used the AD mouse Shionogi tumor model that shares similar characteristics with human prostate cancer. Like human prostate cancer, Shionogi tumors have a functional androgen receptor, undergo extensive castration-induced apoptosis after androgen withdrawal, and later recur as AI tumors in a highly reproducible manner. At the molecular level, the Shionogi tumor model also shares a number of characteristics with human prostate cancers, such as up-regulation of Bcl-2, TRPM-2, and IGFBPs after castration (19, 23, 25). In the present study, we confirmed that the up-regulation of IGFBP-5 after castration is maintained in rapidly growing recurrent AI Shionogi tumors, which along with accelerated growth of IGFBP-5-overexpressing LNCaP tumors, identifies IGFBP-5 overexpression as a potential mediator of progression in this model.

Antisense ODNs, chemically modified stretches of single-stranded DNA that are complementary to mRNA regions of a target gene and thereby effectively inhibit gene expression by forming RNA/DNA duplexes (32), offer one strategy to specifically target *IGFBP-5* gene expression. Phosphorothioate ODNs are water soluble, stable agents manufactured to resist nuclease digestion. After parenteral administration, phosphorothioate ODNs become associated with high-capacity, low-affinity serum binding proteins (33). In this study, phosphorothioate antisense IGFBP-5 ODN corresponding to the mouse *IGFBP-5* translation initiation site was used that inhibited expression of IGFBP-5 mRNA in Shionogi tumor cells in a dose-dependent and sequence-specific manner. Furthermore, antisense IGFBP-5 ODN inhibited cell proliferation and induced cell cycle arrest in Shionogi tumor cells in a time- and dose-dependent manner. Antisense IGFBP-5 ODN treatment did not appear to induce apoptosis either *in vitro* or *in vivo*, which suggests that antisense IGFBP-5 ODN activity

occurs via inhibition of cell proliferation rather than induction of apoptosis. We subsequently showed that the growth-inhibitory effects of antisense IGFBP-5 ODN could be overcome by exogenous IGF-I and that antisense IGFBP-5 ODN treatment caused no additional inhibition of cell proliferation when IGF-I activity was neutralized by anti-IGF-I antibody. We also identified a direct association between cell growth rate and MAPK activity in Shionogi cells after antisense IGFBP-5 ODN treatment. Collectively, these findings demonstrate that antisense IGFBP-5 ODN inhibited the cell proliferation, at least in part, through an IGF-I-dependent mechanism involving inactivation of MAPK.

On the basis of the present *in vitro* data, we hypothesized that targeting IGFBP-5 up-regulation precipitated by androgen withdrawal using antisense strategy may inhibit progression to androgen independence by inhibiting IGFBP-5-enhanced IGF-I activity. In our *in vivo* experiments, administration of antisense IGFBP-5 ODN after castration delayed time to AI progression and inhibited AI recurrent tumor growth. Consistent with our *in vitro* treatments, treatment of mice bearing Shionogi tumors with antisense IGFBP-5 ODN also inhibited the IGFBP-5 mRNA expression *in vivo*. These findings illustrate that *in vivo* systemic administration of ODN can result in sequence-specific down-regulation of a target gene in tumor tissues.

As described above, the biological activity of IGFBP-5 varies depending upon various cell types, which may reflect differential regulation of extracellular matrix interactions (3, 4, 29, 30) or posttranslational modification (31). Indeed, even cell growth conditions will significantly affect IGFBP-5 expression, as shown in Shionogi cells grown *in vitro* (high expressing) versus AD tumors *in vivo* (no expression). Therefore, although our present data show that IGFBP-5 enhances IGF-I bioactivity and increases cell proliferation, studies using additional prostate tumor systems (34, 35) are needed to clarify tissue-specific interactions between IGF-I and IGFBP-5 and to better define the relative importance of IGFBP-5 after androgen ablation in prostate cancer.

A rational strategy to delay AI progression should be based on molecular mechanisms and would target the adaptive changes in gene expression precipitated by androgen withdrawal, rather than the conventional approach of treating patients with established hormone refractory disease. Integration and appropriate timing of combination therapies, based on biological mechanism of progression and castration-induced changes in gene expression, may provide means to inhibit AI progression in a major way. The present study provides the first direct evidence to support a functional role for IGFBP-5 in AI progression. Dramatic up-regulation of IGFBP-5 after castration helps potentiate the mitogenic activity of IGF-I. Furthermore, reduction of IGFBP-5 gene expression using antisense IGFBP-5 ODN delays recurrence and growth of AI tumors. These preclinical data identify a novel target and therapy using antisense IGFBP-5 ODN after androgen ablation in patients with advanced prostate cancer.

ACKNOWLEDGMENTS

We thank Mary Bowden and Virginia Yago for excellent technical assistance.

REFERENCES

1. Denis, L., and Murphy, G. P. Overview of Phase III trials on combined androgen treatment in patients with metastatic prostate cancer. *Cancer (Phila.)*, 72: 3888–3895, 1993.
2. Oh, W. K., and Kantoff, P. W. Management of hormone refractory prostate cancer: current standards and future prospects. *J. Urol.*, 160: 1220–1229, 1998.
3. Jones, J. I., and Clemmons, D. R. Insulin-like growth factors and their binding proteins: biological actions. *Endocr. Rev.*, 16: 3–34, 1995.
4. Rajaram, S., Baylink, D. J., and Mohan, S. Insulin-like growth factor-binding proteins in serum and other biological fluids: regulation and functions. *Endocr. Rev.*, 18: 801–831, 1997.
5. Andress, D., and Birnbaum, R. Human osteoblast-derived insulin-like growth factor (IGF) binding protein-5 stimulates osteoblast mitogenesis and potentiates IGF actions. *J. Biol. Chem.*, 267: 22467–22472, 1992.
6. Huynh, H. T., Yang, X., and Pollak, M. Estradiol and antiestrogens regulate a growth inhibitory insulin-like growth factor binding protein 3 autocrine loop in human breast cancer cells. *J. Biol. Chem.*, 271: 1016–1021, 1996.
7. Damon, S. E., Maddison, L., Ware, J. L., and Plymate, S. R. Overexpression of an inhibitory insulin-like growth factor binding protein (IGFBP), IGFBP-4, delays onset of prostate tumor formation. *Endocrinology*, 139: 3456–3464, 1998.
8. Oh, Y., Muller, H. L., Lamson, G., and Rosenfeld, R. G. Insulin-like growth factor (IGF)-independent action of IGF-binding protein-3 in Hs578T human breast cancer cells. *J. Biol. Chem.*, 268: 14964–14971, 1993.
9. Elgin, R. G., Busby, W. H., and Clemmons, D. R. An insulin-like growth factor (IGF) binding protein enhances the biological response to IGF-I. *Proc. Natl. Acad. Sci. USA*, 84: 3254–3258, 1987.
10. Sprenger, C. C., Damon, S. E., Hwa, V., Rosenfeld, R. G., and Plymate, S. R. Insulin-like growth factor binding protein-related protein 1 (IGFBP-rP1) is a potential tumor suppressor protein for prostate cancer. *Cancer Res.*, 59: 2370–2375, 1999.
11. Boudon, C., Rodier, G., Lechevallier, E., Mottet, N., Barenton, N., and Sultan, C. Secretion of insulin-like growth factors and their binding proteins by human normal and hyperplastic prostatic cells in primary culture. *J. Clin. Endocrinol. Metab.*, 81: 612–617, 1996.
12. Angelloz-Nicoud, P., and Binoux, M. Autocrine regulation of cell proliferation by the insulin-like growth factor (IGF) and IGF binding protein-3 protease system in a human prostate carcinoma cell line. *Endocrinology*, 136: 5485–5492, 1995.
13. Nickerson, T., Pollak, M., and Huynh, H. Castration-induced apoptosis in the rat ventral prostate is associated with increased expression of genes encoding insulin-like growth factor binding proteins 2, 3, 4 and 5. *Endocrinology*, 139: 807–810, 1998.
14. Thomas, L. N., Cohen, P., Douglas, R. C., Lazier, C., and Rittmaster, R. S. Insulin-like growth factor binding protein 5 is associated with involution of the ventral prostate in castrated and finasteride-treated rats. *Prostate*, 35: 273–278, 1998.
15. Nickerson, T., and Pollak, M. Bicaltamide-induced prostate regression involves increased expression of genes encoding insulin-like growth factor binding proteins. *Urology*, 54: 1120–1151, 1999.
16. Huynh, H., Pollak, M., and Zhang, J. Regulation of IGF-II and IGFBP-3 autocrine loop in human PC-3 prostate cancer cells by vitamin D metabolite 1,25(OH)₂D₃ and its analogue EB1089. *Int. J. Oncol.*, 13: 137–143, 1998.
17. Huynh, H., Seyam, R. M., and Brock, G. B. Reduction of ventral prostate weight by finasteride is associated with suppression of insulin-like growth factor I (IGF-I) and IGF-I receptor genes and with an increase in IGF binding protein 3. *Cancer Res.*, 58: 215–218, 1998.
18. Figueroa, J. A., De Raad, S., Tadlock, L., Speights, V. O., and Rinehart, J. J. Differential expression of insulin-like growth factor binding proteins in high versus low Gleason score prostate cancer. *J. Urol.*, 159: 1379–1383, 1998.
19. Miyake, H., Tolcher, A., and Gleave, M. E. Antisense Bcl-2 oligodeoxynucleotides inhibit progression to androgen-independence after castration in the Shionogi tumor model. *Cancer Res.*, 59: 4030–4034, 1999.
20. Gleave, M. E., Hsieh, J. T., Gao, C., von Eschenbach, A. C., and Chung, L. W. K. Acceleration of human prostate carcinoma growth *in vivo* by factors produced by prostate and bone fibroblasts. *Cancer Res.*, 51: 3753–3761, 1991.
21. Pollak, M., Beamer, W., and Zhang, J. Insulin-like growth factors and prostate cancer. *Cancer Metastasis Rev.*, 17: 383–390, 1999.
22. Miyake, H., Hanada, N., Nakamura, H., Kagawa, S., Fujiwara, T., Hara, I., Eto, H., Gohji, K., Arakawa, S., Kamidono, S., and Saya, H. Overexpression of Bcl-2 in bladder cancer cells inhibits apoptosis induced by cisplatin and adenoviral-mediated p53 gene transfer. *Oncogene*, 16: 933–943, 1998.
23. Rennie, P. S., Bruchovsky, N., Buttyan, R., and Cheng, H. Gene expression during the early phase of regression of the androgen-dependent Shionogi mouse mammary carcinoma. *Cancer Res.*, 48: 6309–6312, 1988.
24. Bruchovsky, N., and Rennie, P. S. Classification of dependent and autonomous variants of Shionogi mammary carcinoma based on heterogeneous patterns of androgen binding. *Cell*, 13: 272–280, 1978.
25. Nickerson, T., Miyake, H., Gleave, M. E., and Pollak, M. Castration-induced apoptosis of androgen-dependent Shionogi carcinoma is associated with increased expression of genes encoding insulin-like growth factor binding proteins. *Cancer Res.*, 59: 3392–3395, 1999.
26. Pietrkowski, Z., Mulholland, G., Gomella, L., Jameson, B. A., Wernicke, D., and Baserga, R. Inhibition of growth of prostatic cell lines by peptide analogues of insulin-like growth factors. *Cancer Res.*, 53: 1102–1108, 1993.
27. Wolk, A., Mantzoros, C. S., Andersson, S. O., Bergstrom, R., Signorello, L. B., Lagiou, P., Adami, H. O., and Trichopoulos, D. Insulin-like growth factor I and prostate cancer risk: a population-based, case-control study. *J. Natl. Cancer Inst.*, 90: 911–915, 1998.
28. Conover, C. A., Bale, L. K., Clarkson, J. T., and Topping, O. Regulation of insulin-like growth factor binding protein-5 messenger ribonucleic acid expression and protein availability in rat osteoblast-like cells. *Endocrinology*, 132: 2525–2530, 1993.
29. Arai, T., Arai, A., Busby, W. H., Jr., and Clemmons, D. R. Glycosaminoglycans inhibit degradation of insulin-like growth factor-binding protein-5. *Endocrinology*, 135: 2358–2363, 1994.
30. Jones, J. I., Gockerman, A., Busby, W. H., Jr., Camacho-Hubner, C., and Clemmons, D. R. Extracellular matrix contains insulin-like growth factor binding protein-5: potentiation of the effects of IGF-I. *J. Cell Biol.*, 121: 679–687, 1993.
31. Andress, D. L., Loop, S. M., Zapf, J., and Kiefer, M. C. Carboxytruncated insulin-like growth factor binding protein-5 stimulates mitogenesis in osteoblast-like cells. *Biochem. Biophys. Res. Commun.*, 195: 25–30, 1993.
32. Crooke, S. T. Therapeutic applications of oligonucleotides. *Annu. Rev. Pharmacol. Toxicol.*, 32: 329–376, 1993.
33. Saijo, Y., Perlaky, L., Wang, H., and Busch, H. Pharmacokinetics, tissue distribution, and stability of antisense oligodeoxynucleotide phosphorothioate ISIS 3466 in mice. *Oncol. Res.*, 6: 243–249, 1994.
34. Gregory, C. W., Kim, D., Ye, P., D'Ercole, A. J., Pretlow, T. G., Mohler, J. L., and French, F. S. Androgen receptor up-regulates insulin-like growth factor binding protein-5 (IGFBP-5) expression in a human prostate cancer xenograft. *Endocrinology*, 140: 2372–2381, 1999.
35. Klein, K. A., Reiter, R. E., Moradi, H., Zhu, X. L., Brothman, A. R., Lamb, D. J., Marcelli, M., Belldedegum, A., Witte, O. N., and Sawyers, C. L. Progression of metastatic human prostate cancer to androgen independence in immunodeficient SCID mice. *Nat. Med.*, 3: 402–408, 1997.

Cancer Research

The Journal of Cancer Research (1916–1930) | The American Journal of Cancer (1931–1940)

Castration-induced Up-Regulation of Insulin-like Growth Factor Binding Protein-5 Potentiates Insulin-like Growth Factor-I Activity and Accelerates Progression to Androgen Independence in Prostate Cancer Models

Hideaki Miyake, Michael Pollak and Martin E. Gleave

Cancer Res 2000;60:3058-3064.

Updated version Access the most recent version of this article at:
<http://cancerres.aacrjournals.org/content/60/11/3058>

Cited articles This article cites 34 articles, 12 of which you can access for free at:
<http://cancerres.aacrjournals.org/content/60/11/3058.full#ref-list-1>

Citing articles This article has been cited by 21 HighWire-hosted articles. Access the articles at:
<http://cancerres.aacrjournals.org/content/60/11/3058.full#related-urls>

E-mail alerts [Sign up to receive free email-alerts](#) related to this article or journal.

Reprints and Subscriptions To order reprints of this article or to subscribe to the journal, contact the AACR Publications Department at pubs@aacr.org.

Permissions To request permission to re-use all or part of this article, use this link
<http://cancerres.aacrjournals.org/content/60/11/3058>.
Click on "Request Permissions" which will take you to the Copyright Clearance Center's (CCC) Rightslink site.